THE JOURNAL OF PHYSICAL CHEMISTRY A

pubs.acs.org/JPCA Article

Angular Dependence of Strong Field Ionization of 2-Phenylethyl-*N*,*N*-dimethylamine (PENNA) Using Time-Dependent Configuration Interaction with an Absorbing Potential

Paul Hoerner, Wen Li, and H. Bernhard Schlegel*

Cite This: https://dx.doi.org/10.1021/acs.jpca.0c03438 Read Online

ACCESS | Metrics & More | Article Recommendations

ABSTRACT: Ionization of 2-phenylethyl-*N*,*N*-dimethylamine (PENNA) may lead to charge migration between the amine group and the phenyl group. The angular dependence of strong field ionization of PENNA has been modeled by time-dependent configuration interaction with an absorbing potential. The total ionization rate can be partitioned into contributions from the amine group and the phenyl group, and these components have very distinct shapes. Ionization from the amine is primarily from the side opposite to the lone pair and is dominated by the CH_2 and CH_3 groups. Similarly, trimethylamine ($N(CH_3)_3$), dimethyl ether (CH_3OCH_3), and methyl fluoride (CH_3F) are also found to ionize primarily from the methyl groups. The predominance of ionization from the methyl groups can be attributed to the fact that the orbital energies of individual lone pairs of N, O, and F are lower than the CH_3 groups. Because the angular dependence of ionization of the two groups is quite different, alignment of PENNA could be used to control the ratio of the amine and phenyl cations and potentially probe charge migration in PENNA cation.

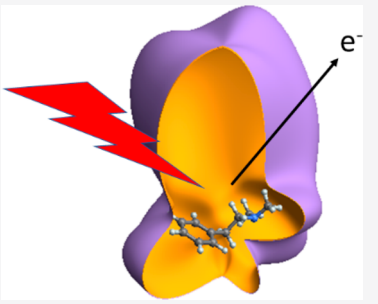

INTRODUCTION

PENNA is a bifunctional molecule consisting of a phenyl group and an amine separated by an ethyl spacer. The highest occupied molecular orbitals (HOMO, HOMO−1, and HOMO−2) are localized on these two functional groups in neutrals while the charge density is delocalized in cations. Due to this unique electronic structure, a local ionization from either group can lead to a coherent superposition of two cation states which initially localizes charge density on one side of the molecule. As an example of a coherent electronic process in the first few femtoseconds, the ensuing charge oscillation (charge migration) between phenyl and amine groups has attracted much attention in the past two decades.[1−11] Theoretical studies typically start with a superposition of cation states, approximated by a sudden ionization, and then track charge migration by monitoring the charge or spin density. Whether this approximation is realistic for PENNA has not been assessed experimentally and there have been no reports of charge migration in PENNA so far. This could be due to competition between charge migration and decoherence when nuclear motion is included in the theoretical simulations.[8,9,11] In the present study, we have modeled the initial ionization process of PENNA driven by a strong laser field, which is a major method for producing and probing electronic coherence. Specifically, we have examined the molecular frame angular dependence of this ionization process.

For sufficiently strong fields, ionization can occur by tunneling through the Coulomb barrier or by barrier suppression. In previous studies we have used time-dependent configuration interaction with a complex absorbing potential (TDCI-CAP) to simulate strong field ionization.[12−22] This has revealed a strong angular dependence for the ionization rate. For small, high symmetry molecules, the shape of the frontier orbitals dictates the angular dependence of ionization. In the present study, we have used the TDCI-CAP approach to study the strong field ionization of PENNA and examine the orbital contributions to the angular dependence of the ionization yield.

METHODS

To simulate ionization in a strong field, the electronic wave function was propagated with the time-dependent Schrödinger equation:

$$i\frac{\partial}{\partial t}\Psi_{el}(t) = [\hat{\mathbf{H}}_{el} - \vec{\hat{\mu}}\cdot\vec{E}(t) - i\bar{\mathbf{V}}^{absorb}]\Psi_{el}(t) \quad (1)$$

$$\Psi_{el}(t) = \sum_{i=0} C_i(t)|\Psi_i\rangle \quad (2)$$

Received: April 17, 2020
Revised: May 18, 2020
Published: May 19, 2020

where $\hat{H}_{el}$ is the field-free electronic Hamiltonian (atomic units are used throughout the paper). The Hartree−Fock ground state and all singly excited states of the field-free and time-independent Hamiltonian were used as a basis for the time-dependent wave function. The interaction with the intense electric field was treated in the semiclassical dipole approximation, where $\hat{\vec{\mu}}$ is the dipole operator and $\vec{E}$ is the electric field. As described in our previous papers,[12−20] ionization was modeled with a complex absorbing potential (CAP), $-i\hat{V}^{absorb}$. The total absorbing potential for the molecule is equal to the minimum of the values of spherical absorbing potentials centered on each atom. Each spherical potential begins at 3.5 times the van der Waals radius of each element (R_H = 9.544 bohr, R_C = 12.735 bohr, and R_N = 12.104 bohr), rises quadratically to 5 hartree at approximately R + 14 bohr and turns over quadratically to 10 hartree at approximately R + 28 bohr. To obtain directional information for ionization, a static field was used instead of an oscillating field.[18,20,21] To prevent nonadiabatic excitations, the electric field was ramped up slowly to a constant value:

$$E(t) = E_{max}\left(1 - \left(1 - \frac{3}{2}\frac{t}{t_{max}}\right)^4\right) \text{ for } 0 \le t \le \frac{2}{3}t_{max},$$

$$E(t) = E_{max} \quad \text{for } t \ge \frac{2}{3}t_{max} \tag{3}$$

where E_{max} is the maximum field strength and t_{max} = 800 au = 19.35 fs is the total propagation time. The ionization rate was calculated by taking average of the instantaneous rates from t = 12.88 to 19.35 fs. Trotter factorization of the exponential of the Hamiltonian is used to propagate the time-dependent wave function:

$$\Psi(t + \Delta t) = \exp(-i\bar{\mathbf{H}}\Delta t)\Psi(t)$$

$$\begin{aligned}\mathbf{C}(t + \Delta t) = {} & \exp(-i\mathbf{H}_{el}\Delta t/2)\exp(-\mathbf{V}^{absorb}\Delta t/2)\mathbf{W}^T \\ & \exp(iE(t + \Delta t/2)\mathbf{d}\Delta t)\mathbf{W} \\ & \exp(-\mathbf{V}^{absorb}\Delta t/2)\exp(-i\mathbf{H}_{el}\Delta t/2)\mathbf{C}(t)\end{aligned} \tag{4}$$

Since Ψ is expanded in terms of the states of the field-free Hamiltonian, $\mathbf{H}_{el}$ is a diagonal matrix and $\exp(-i\mathbf{H}_{el}\Delta t/2)$ is easy to obtain and needs to be calculated only once at the beginning of the propagation. Because the absorbing potential is independent of time, $\exp(-\mathbf{V}^{absorb}\Delta t/2)$ also needs to be calculated only once and is obtained by using the eigenvalues and eigenvectors of the full matrix $\mathbf{V}^{absorb}$. For a given linearly polarized pulse, the field amplitude $E(t)$ varies in time but the field direction is constant. To calculate the interaction with the laser field, $\mathbf{D}$, the dipole moment matrix for the given field direction is diagonalized, $\mathbf{WDW}^T = \mathbf{d}$, in order to calculate the exponential $\exp(iE(t + \Delta t/2)\mathbf{D}\Delta t) = \mathbf{W}^T \exp(iE(t + \Delta t/2)\mathbf{d}\Delta t)\mathbf{W}$. The diagonal matrix $\exp(iE(t + \Delta t/2)\mathbf{d}\Delta t)$ is the only component of the Trotter factorization that varies with time and easily calculated at each time step. The numerical work can be reduced further by forming the product $\mathbf{U} = \exp(-\mathbf{V}^{absorb}\Delta t/2)\ \mathbf{W}^T$ at the beginning of the propagation. Thus, each propagation step requires two full matrix-vector products (involving $\mathbf{U}$ and $\mathbf{U}^T$) and three diagonal matrix-vector products (involving $\exp(-i\mathbf{H}_{el}\Delta t/2)$ and $\exp(iE(t + \Delta t/2)\mathbf{d}\Delta t)$). Because the propagation uses the exponential of the Hamiltonian, a fairly large time step of Δt = 0.05 au (1.2 as) can used. In similar simulations,[18] reducing the time step by a factor of 2 changed the norm at the end of the propagation by less than 0.01%.

A locally modified version of the Gaussian software package[23] was used to calculate the integrals needed for the TDCIS-CAP simulation. The Dunning aug-cc-pVTZ basis set[24] was augmented with a set of additional diffuse functions placed on each atom (three s functions with exponents of 0.0256, 0.0128, and 0.0064; three p functions with exponents of 0.0256, 0.0128, and 0.0064; three d functions with exponents of 0.0512, 0.0256, and 0.0128; and one f function with an exponent of 0.0256)[12,18] for adequate interaction with the CAP. The TDCIS-CAP simulations included all singly excited configurations with an excitation energy of less than 10.00 hartree for a total of 22741 states. The TDCIS simulations were carried out with an external Fortran95 code. The angle-dependent ionization rates were calculated for 62 directions (steps of 30° in spherical angles θ and φ) and fitted to polynomials in $\cos(\theta)^n \cos(m\varphi)$ and $\cos(\theta)^n \sin(m\varphi)$, n = 0−7, m = 0−6 to obtain smooth surfaces for plotting. Mulliken population analysis of the normalized one electron density of the absorbed wave function, $\hat{V}^{absorb}\Psi_{el}(t)$ was used to partition the total ionization rate into contributions from individual orbitals.

RESULTS AND DISCUSSION

The angle dependent strong field ionization rate for PENNA is shown in Figure 1 for a field strength of 0.04 au, which corresponds to 2.1 V/Å. The loss of norm ranges from 8% to 46% and the rates range from 0.01−0.09 e/fs. The large lobe is

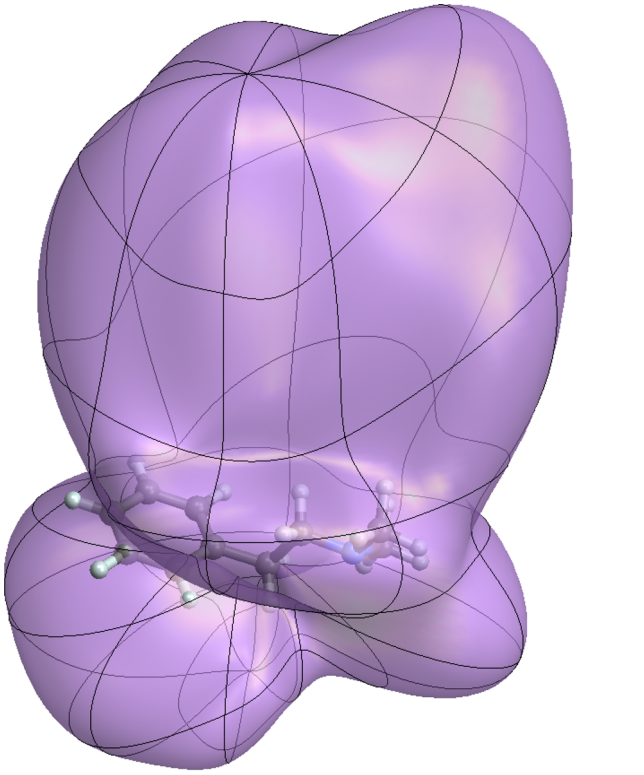

Figure 1. Ionization rate for PENNA in a static field of 0.04 au (2.1 V/Å). Distance from the center is proportional to the ionization rate and the direction corresponds to the direction the electron is ejected (i.e., minus the electric field).

https://dx.doi.org/10.1021/acs.jpca.0c03438
J. Phys. Chem. A XXXX, XXX, XXX−XXX

primarily due to ionization of the amine group. The node parallel to the plane of phenyl ring corresponds to the node in the highest occupied π orbitals of the benzene ring.

More specific information about the orbital contributions can be obtained by using the population analysis of the absorbed wave function to partition the total ionization rate. Figure 2 shows the angular dependence of the contributions

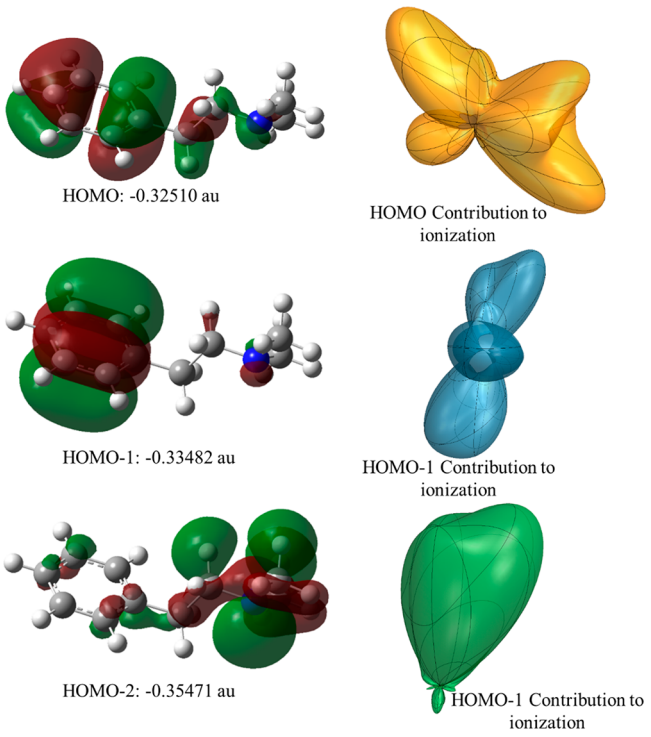

Figure 2. Highest occupied molecular orbitals for PENNA and their contributions to the angular dependence of the strong field ionization rate shown in Figure 1.

from HOMO, HOMO−1, and HOMO−2. For Hartree−Fock calculations, energies of π orbitals centered on phenyl group are ε = −0.321, −0.330 hartree, and energies for orbital centered on the amine group is ε = −0.355 hartree. For density functional calculations with ωB97XD,[25] the energies for the highest occupied orbitals are ε = −0.294 hartree for the amine group and ε = −0.321, −0.330 hartree for the phenyl group. Nodal structure of orbitals is reflected in the shape of the ionization yield from these orbitals. The regions of PENNA contributing to the ionization can be deduced from the molecular orbitals and the magnitudes of their contributions to the angular dependence of the total ionization are shown in the same orientation next to each orbital. The contributions from phenyl π orbitals are similar to angular dependence of ionization for the two highest occupied orbitals in benzene showing a node in the plane of the ring and a node perpendicular to the ring. The orbital on the amine group consists of a nitrogen lone pair antibonding with neighboring alkyl groups. This orbital makes the largest contribution to the total ionization rate. The remaining lower energy orbitals do not contribute significantly to ionization.

Curiously, the contribution of the amine group to the total ionization is primarily from the back side of the nitrogen lone pair. The strong field ionization of two simple molecules with nitrogen lone pair orbitals shown in Figure 3 provide some

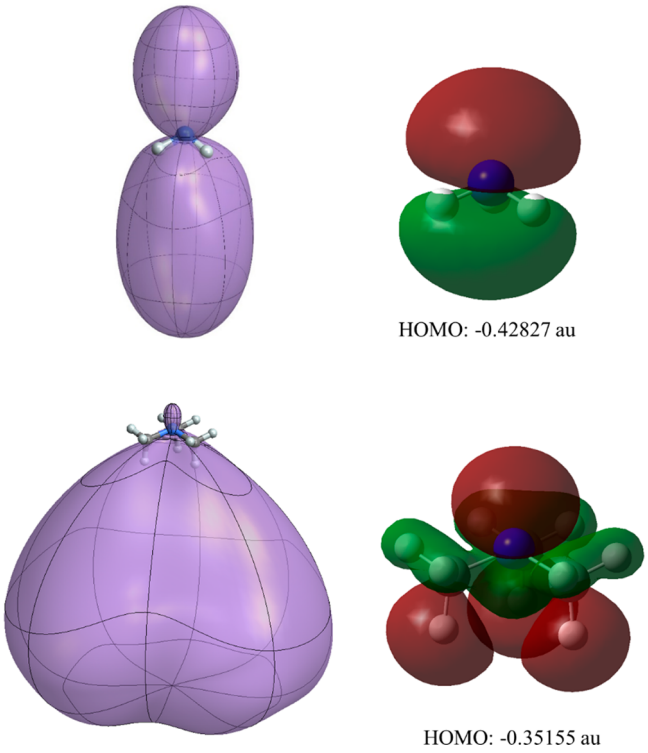

Figure 3. Highest occupied molecular orbitals for NH_3 and $N(CH_3)_3$ and the angular dependence of the ionization rates in static fields of 0.05 au (2.6 V/Å) and 0.04 au (2.1 V/Å), respectively. The maximum losses of norm are 41% and 69%, respectively.

understanding of this directionality. For ammonia, the HOMO is a nitrogen lone pair orbital interacting with the NH bonding orbitals in an out-of-phase manner. The angular dependence of ionization shows nearly equal parts from the nitrogen lone pair and from the NH bonds. Trimethylamine, $N(CH_3)_3$, is a better model for the amine group in PENNA. The HOMO consists of nitrogen lone pair in an out-of-phase combination with the CH bonds of the three methyl groups. Because frontier orbitals for the methyl group are higher in energy than the energies of isolated nitrogen lone pair, the methyl groups form the larger component of the HOMO and contribute strongly to the ionization. Since the ionization potential for a methyl group (e.g., propane IP = 10.94 eV, isobutane IP = 10.68 eV) is considerably lower than the ionization potential for nitrogen (14.53 eV for nitrogen atom), most of the ionization in trimethylamine comes from the methyl groups. As a result, the highest ionization rate is in the direction opposite to the nitrogen lone pair.

Similar angular dependence of strong field ionization can be seen in CH_3OCH_3 and CH_3F shown in Figure 4. The effect is somewhat more extreme than in $N(CH_3)_3$ because the greater electronegativity of O and F. Even though HOMO's of CH_3OCH_3 and CH_3F have sizable contributions from the O and F lone pairs, the angular dependence of ionization yield is dominated by ionization from the methyl group. Like for $N(CH_3)_3$, this can be attributed to the fact that the frontier orbitals for the methyl group are higher in energy than the energies of isolated O and F lone pair orbitals.

The strong field ionization of PENNA can lead to the coherent superposition of cation states and possibly charge migration. Figure 2 shows that ionization from the amine orbital has a much different angular dependence than

https://dx.doi.org/10.1021/acs.jpca.0c03438
J. Phys. Chem. A XXXX, XXX, XXX−XXX

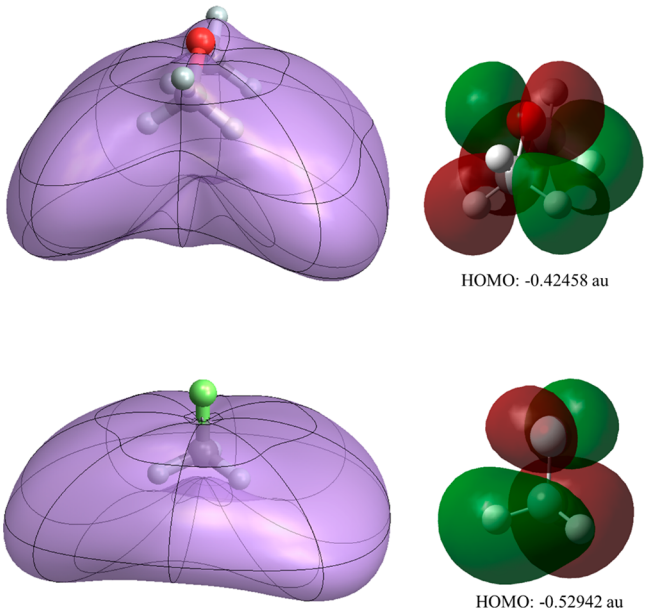

Figure 4. Highest occupied molecular orbitals for CH_3OCH_3 and CH_3F and angular dependence of the ionization rate in static fields of 0.06 au (3.1 V/Å) and 0.075 au (3.9 V/Å), respectively. The maximum losses of norm are 73% and 75%, respectively.

ionization from the phenyl orbitals. Consequently, the ratio of amine to phenyl cations has a very pronounced angular dependence, as shown in Figure 5. This in turn could affect the

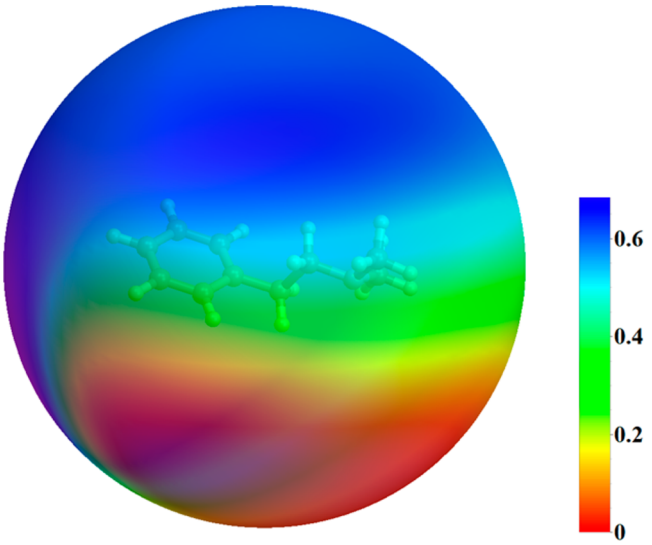

Figure 5. Angular dependence of the ratio of amine ionization to the total ionization (blue is mainly amine ionization, and yellow and red are mainly phenyl ionization).

nature of the charge migration. However, the current study does not calculate the coherence among different cation states and therefore it is not straightforward to study the charge migration process. This will be addressed in future work.

SUMMARY

Time-dependent configuration interaction with single excitations and a complex absorbing potential has been used to simulate strong field ionization of PENNA. A static field was slowly ramped up and held constant at 0.04 au (2.1 V/Å) to obtain ionization rates as a function of the direction of the applied field. Population analysis of the absorbed/ionized wave function was used to partition the total ionization rate into contributions from individual orbitals. The contributions from the phenyl and amine groups have very distinct shapes that correspond qualitatively to the shapes of the highest occupied orbitals of these groups. For the amine group, ionization occurs mainly from the side opposite to the nitrogen lone pair. Trimethylamine is a very close model of the amine group in PENNA and was also found to ionize primarily from the side opposite to the lone pair. Similarly, dimethyl ether and methyl fluoride ionize from the methyl groups rather than from the lone pairs of the electronegative atoms. Because the energies of the CH_3 group orbitals are higher than the energies of the lone pair orbitals of N, O and F, the ionization rate is higher for the methyl groups. If PENNA can be aligned, then the direction of a strong field ionizing pulse can be used to control the ratio of amine to phenyl cations and possibly probe charge migration in PENNA cation.

AUTHOR INFORMATION

Corresponding Author

H. Bernhard Schlegel − *Department of Chemistry, Wayne State University, Detroit, Michigan 48202, United States;* orcid.org/0000-0001-7114-2821; Phone: 313-577-2562; Email: hbs@chem.wayne.edu; Fax: 313-577-8822

Authors

Paul Hoerner − *Department of Chemistry, Wayne State University, Detroit, Michigan 48202, United States*

Wen Li − *Department of Chemistry, Wayne State University, Detroit, Michigan 48202, United States;* orcid.org/0000-0002-3721-4008

Complete contact information is available at: https://pubs.acs.org/10.1021/acs.jpca.0c03438

Notes

The authors declare no competing financial interest.

ACKNOWLEDGMENTS

The authors thank Wayne State University computing grid for the computational time. This work was supported by a grant from National Science Foundation (CHE1856437).

REFERENCES

(1) Weinkauf, R.; Lehr, L.; Metsala, A. Local ionization in 2-phenylethyl-NN-dimethylamine: Charge transfer and dissociation directly after ionization. *J. Phys. Chem. A* **2003**, *107*, 2787−2799.

(2) Cheng, W.; Kuthirummal, N.; Gosselin, J. L.; Solling, T. I.; Weinkauf, R.; Weber, P. M. Control of local ionization and charge transfer in the bifunctional molecule 2-phenylethyl-N, N-dimethylamine using Rydberg fingerprint spectroscopy. *J. Phys. Chem. A* **2005**, *109*, 1920−1925.

(3) Lehr, L.; Horneff, T.; Weinkauf, R.; Schlag, E. W. Femtosecond dynamics after ionization: 2-Phenylethyl-N, N-dimethylamine as a model system for nonresonant downhill charge transfer in peptides. *J. Phys. Chem. A* **2005**, *109*, 8074−8080.

(4) Lunnemann, S.; Kuleff, A. I.; Cederbaum, L. S. Charge migration following ionization in systems with chromophore-donor and amine-acceptor sites. *J. Chem. Phys.* **2008**, *129*, 104305.

(5) Lunnemann, S.; Kuleff, A. I.; Cederbaum, L. S. Ultrafast charge migration in 2-phenylethyl-N, N-dimethylamine. *Chem. Phys. Lett.* **2008**, *450*, 232−235.

https://dx.doi.org/10.1021/acs.jpca.0c03438
J. Phys. Chem. A XXXX, XXX, XXX−XXX

(6) Kuleff, A. I.; Dreuw, A. Theoretical description of charge migration with a single Slater-determinant and beyond. *J. Chem. Phys.* **2009**, *130*, 034102.
(7) Gomez-Carrasco, S.; Koppel, H. Quantum dynamical study of low-energy photoelectron bands of 2-phenylethyl-N, N-dimethyl-amine. *J. Chem. Sci.* **2012**, *124*, 247−253.
(8) Mignolet, B.; Levine, R. D.; Remacle, F. Charge migration in the bifunctional PENNA cation induced and probed by ultrafast ionization: a dynamical study. *J. Phys. B: At., Mol. Opt. Phys.* **2014**, *47*, 124011.
(9) Jenkins, A. J.; Vacher, M.; Bearpark, M. J.; Robb, M. A. Nuclear spatial delocalization silences electron density oscillations in 2-phenyl-ethyl-amine (PEA) and 2-phenylethyl-N, N-dimethylamine (PENNA) cations. *J. Chem. Phys.* **2016**, *144*, 104110.
(10) Fan, L.; Lee, S. K.; Tu, Y. J.; Mignolet, B.; Couch, D.; Dorney, K.; Nguyen, Q.; Wooldridge, L.; Murnane, M.; Remacle, F.; et al. A new electron-ion coincidence 3D momentum-imaging method and its application in probing strong field dynamics of 2-phenylethyl-N, N-dimethylamine. *J. Chem. Phys.* **2017**, *147*, 013920.
(11) Sun, S. T.; Mignolet, B.; Fan, L.; Li, W.; Levine, R. D.; Remacle, F. Nuclear Motion Driven Ultrafast Photodissociative Charge Transfer of the PENNA Cation: An Experimental and Computational Study. *J. Phys. Chem. A* **2017**, *121*, 1442−1447.
(12) Krause, P.; Sonk, J. A.; Schlegel, H. B. Strong field ionization rates simulated with time-dependent configuration interaction and an absorbing potential. *J. Chem. Phys.* **2014**, *140*, 174113.
(13) Krause, P.; Schlegel, H. B. Strong-field ionization rates of linear polyenes simulated with time-dependent configuration interaction with an absorbing potential. *J. Chem. Phys.* **2014**, *141*, 174104.
(14) Krause, P.; Schlegel, H. B. Angle-dependent ionization of small molecules by time-dependent configuration interaction and an absorbing potential. *J. Phys. Chem. Lett.* **2015**, *6*, 2140−2146.
(15) Krause, P.; Schlegel, H. B. Angle-dependent ionization of hydrides AH_n calculated by time-dependent configuration interaction with an absorbing potential. *J. Phys. Chem. A* **2015**, *119*, 10212−10220.
(16) Liao, Q.; Li, W.; Schlegel, H. B. Angle-dependent strong-field ionization of triple bonded systems calculated by time-dependent configuration interaction with an absorbing potential. *Can. J. Chem.* **2016**, *94*, 989−997.
(17) Hoerner, P.; Schlegel, H. B. Angular dependence of ionization by circularly polarized light calculated with time-dependent configuration interaction with an absorbing potential. *J. Phys. Chem. A* **2017**, *121*, 1336−1343.
(18) Hoerner, P.; Schlegel, H. B. Angular Dependence of Strong Field Ionization of CH3X (X = F, Cl, Br, or I) Using Time-Dependent Configuration Interaction with an Absorbing Potential. *J. Phys. Chem. A* **2017**, *121*, 5940−5946.
(19) Winney, A. H.; Lee, S. K.; Lin, Y. F.; Liao, Q.; Adhikari, P.; Basnayake, G.; Schlegel, H. B.; Li, W. Attosecond Electron Correlation Dynamics in Double Ionization of Benzene Probed with Two-Electron Angular Streaking. *Phys. Rev. Lett.* **2017**, *119*, 123201.
(20) Hoerner, P.; Schlegel, H. B. Angular Dependence of Strong Field Ionization of Haloacetylenes HCCX (X = F, Cl, Br, I), Using Time-Dependent Configuration Interaction with an Absorbing Potential. *J. Phys. Chem. C* **2018**, *122*, 13751−13757.
(21) Winney, A. H.; Basnayake, G.; Debrah, D. A.; Lin, Y. F.; Lee, S. K.; Hoerner, P.; Liao, C.; Schlegel, H. B.; Li, W. Disentangling Strong-Field Multielectron Dynamics with Angular Streaking. *J. Phys. Chem. Lett.* **2018**, *9*, 2539−2545.
(22) Hoerner, P.; Lee, M. K.; Schlegel, H. B. Angular dependence of strong field ionization of N-2 by time-dependent configuration interaction using density functional theory and the Tamm-Dancoff approximation. *J. Chem. Phys.* **2019**, *151*, 054102.
(23) Frisch, M. J.; Trucks, G. W.; Schlegel, H. B.; Scuseria, G. E.; et al. *Gaussian Development Version*, revision I.09; Gaussian Inc.: Wallingford, CT, 2010.
(24) Dunning, T. H. Gaussian-basis sets for use in correlated molecular calculations. 1. The atoms boron through neon and hydrogen. *J. Chem. Phys.* **1989**, *90*, 1007−1023.
(25) Chai, J. D.; Head-Gordon, M. Long-range corrected hybrid density functionals with damped atom-atom dispersion corrections. *Phys. Chem. Chem. Phys.* **2008**, *10*, 6615−6620.

https://dx.doi.org/10.1021/acs.jpca.0c03438
J. Phys. Chem. A XXXX, XXX, XXX−XXX